

Research paper

Could network analysis of horizontal visibility graphs be faithfully used to infer long-term memory properties in real-world time series?

Yu Huang, Qimin Deng, Zuntao Fu*

Lab for Climate and Ocean-Atmosphere Studies, Department of Atmospheric and Oceanic Sciences, School of Physics, Peking University, Beijing, 100871, China



ARTICLE INFO

Article history:

Received 27 December 2018

Revised 6 June 2019

Accepted 3 July 2019

Available online 04 July 2019

Keywords:

Long-term memory

Horizontal visibility graph

Topological parameters

Short-term correlation

Nonlinear correlations

ABSTRACT

Mapping time series to complex networks has great potential to investigate their temporal structures. Some previous studies have been carried on time series generated from idealized stochastic models and found that there are inherent associations between long-term memory (LTM) of pure long-range correlated time series and topological parameters (TPs) of their networks, which is thought as a new prospective to extract information from time series. However, output time series from natural systems seldom take so idealized structures as those from idealized stochastic models, and there is usually some unconsidered information inherited in them, which makes these derived associations questionable. To check and generalize these conclusions acquired from idealized stochastic models, horizontal visibility graph (HVG) algorithm is employed to map time series to their horizontal visibility networks. Firstly synthetic time series with known mixed correlations (apart from LTM) have been analyzed and results indicate that topological parameters (TPs) of HVG networks are not solely dominated by the strength of LTM, other factors such as white noise, short-term correlation (STC) and nonlinear correlations are also playing crucial roles. Taking this fact into account, after some preprocessing treatments have been carried out, the LTM of daily mean air temperature series can indeed be inferred by means of the inherent associations between LTM of pure long-range correlated time series and TPs of their networks.

© 2019 Elsevier B.V. All rights reserved.

1. Introduction

A crucial characteristic of stochastic time series is long-term memory (LTM) and it is widely concerned in the fields of hydrology, traffic, biology, economy and climate [1–5], since that LTM is conducive to analyzing and predicting features of the complex systems [4–6]. It is necessary for constantly improved methods to better infer LTM of time series [4,7,8]. Detrended fluctuation analysis [9] (DFA) is the most often-used method [4–8], with the DFA exponent $\alpha \in (0.5, 1)$ for LTM and $\alpha = 0.5$ for no long range memory. However, short-term correlation (STC) [10–13], white noise [12,14], and seasonal cycle [15] often affect estimated LTM by DFA, and in this case the correct scaling range has to be carefully acquired in special intervals.

* Corresponding author.

E-mail address: fuzt@pku.edu.cn (Z. Fu).

In recent years, complex network approaches to time series analysis are demonstrated to be useful in many fields and sometimes even more effective than traditional approaches [16–18]. For example, many time series features can be revealed by topological patterns of complex network, and complex network is often demonstrated robust to noise and data length. Meanwhile LTM of time series is also found to be inherently related to the complex network approaches, and this has attracted many discussions about its possible role on the development of time series analysis and complex network researches [8,18–21]. Especially, Manshour calculated three topological parameters (TPs) of horizontal visibility graph (HVG) and found their values would monotonically decrease with the LTM of time series increasing, which suggested that they could be used to infer LTM strength of the idealized fractional time series [20]. Considering the advantages of complex network revealed in the past researches [18], applying network approach to infer LTM of time series is really a potential scheme, but it is worthy to note that there are different conditions between time series from idealized stochastic models and real-world time series, such as different kinds of noise and some nonlinear structures in time series [22–23]. Here we raise our question, could network analysis of HVG be faithfully used to infer LTM properties in real-world time series?

Apart from LTM, there are some other time series structures may be reflected by complex network approaches to time series. For example, Weng et al. found that there are distinct patterns in the network features from time series with different features such as STC and some period or chaotic dynamics [24]. The study of Zhang also revealed that STC of time series from auto-regressive stochastic processes has important effect on the degree distribution of their HVG [25]. And then recent studies indicated that some nonlinear structures of time series can be detected by HVG [26,27]. These results show that the network properties for the whole time series can be altered by the time series with different dynamics besides LTM. Moreover, for time series from natural systems with different dynamics, it is unknown which process plays its dominated role on the global network properties. The associations between LTM and network TPs from idealized stochastic models or processes may not be simply generalized to study real-world time series. It might be necessary to investigate how these complicated features in time series will influence the quality of detecting LTM by HVG, and if reasonable processing could eliminate the influences.

In this article, we explore how faithfully TPs of HVG can be used to analyze LTM under more complicated conditions, especially for real-world temperature series, where STC, nonlinear correlation (NC), and measured noise (MN) are non-negligible, see Fig. 1b with coexistence of both STC and LTM, and Fig. 1c with dominated NC. Firstly, we generate synthetic time series from stochastic models to see how TPs of HVG are altered by LTM, STC and white noise, and meanwhile we test if these influences could be eliminated by reasonable processing. Then daily mean air temperature series are analyzed to answer the question: Could network analysis of HVG be faithfully used to infer LTM properties in real-world time series? At last, both definite answer to this question and a systematic way to preprocess the time series from the real world to infer its LTM are provided.

2. Data and methods

2.1. Data

In this study, the analyzed real-world time series is the daily mean air temperature series measured at 87 stations over China (Fig. 1a shows their spatial distribution). The data is obtained from the China Meteorological Data sharing Service System (<http://cdc.cma.gov.cn>), with data length of 53 years (1957–2010). For all temperature series analyzed in this paper, the annual cycle has been subtracted in advance. That is to say, the analyzed temperature series are the anomalies $T_i - \langle T_i \rangle$, where T_i is raw records and $\langle T_i \rangle$ is a long-time climatological average for each calendar day of each year.

2.2. Methods

2.2.1. Complex network approach based on HVG

For a given time series $\{x_t\}$ ($t = 1, \dots, N$, N is the size of data length), we transform it into a network by the HVG algorithm [28]. Every data point is taken as a node, and a link can be established between two data points x_a and x_b if they and any intermediate data point x_q follow the criterion:

$$x_a, x_b > x_q \text{ for all } q \text{ that } a < q < b. \quad (1)$$

After this HVG is constructed, we calculate three important network parameters following Manshour's works [20], who found that these three network parameters are associated with the fundamental network's topological characteristics. And more importantly, previous studies show that visibility related algorithm can preserve the ordinal pattern information of the original series in its corresponding degree series. The first one is assortativity coefficient [29]:

$$r = \frac{M^{-1} \sum_i j_i k_i - [M^{-1} \sum_i \frac{1}{2} (j_i + k_i)]^2}{M^{-1} \sum_i \frac{1}{2} (j_i^2 + k_i^2) - [M^{-1} \sum_i \frac{1}{2} (j_i + k_i)]^2}, \quad (2)$$

where M is the total number of links, j_i and k_i are degree number of two nodes in the two ends of i th link. So, this TP is a measure of the Pearson correlation coefficient of nodes in a given link. The second one is the largest Eigen-value (e_{max}) of the adjacent matrix [30], which quantifies the strength of nodes in a graph with their adjacent nodes. The third one is

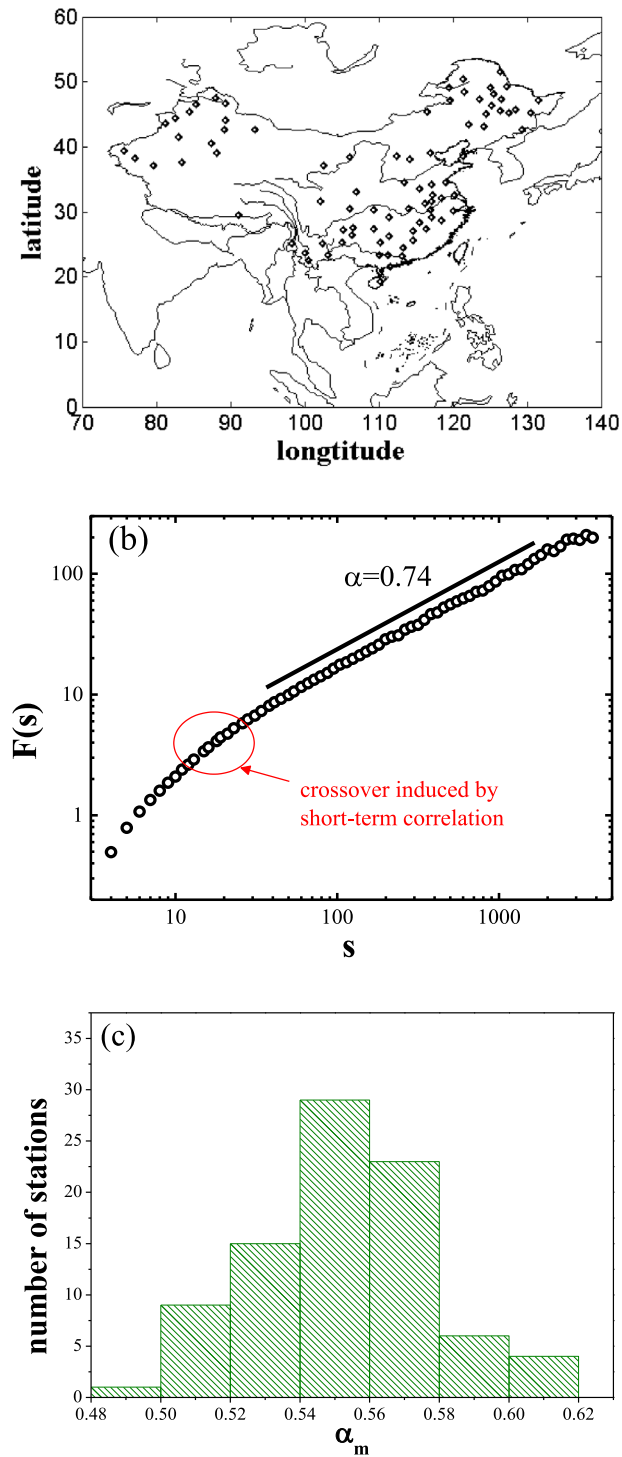


Fig. 1. Details of the mean air temperature series over China: (a) the spatial distribution of stations, (b) DFA result for a representative series over the station Huma and (c) the distribution of α_m for all 87 temperature series (when $0.5 < \alpha_m < 1$, it's considered that there exist nonlinear structures in time series).

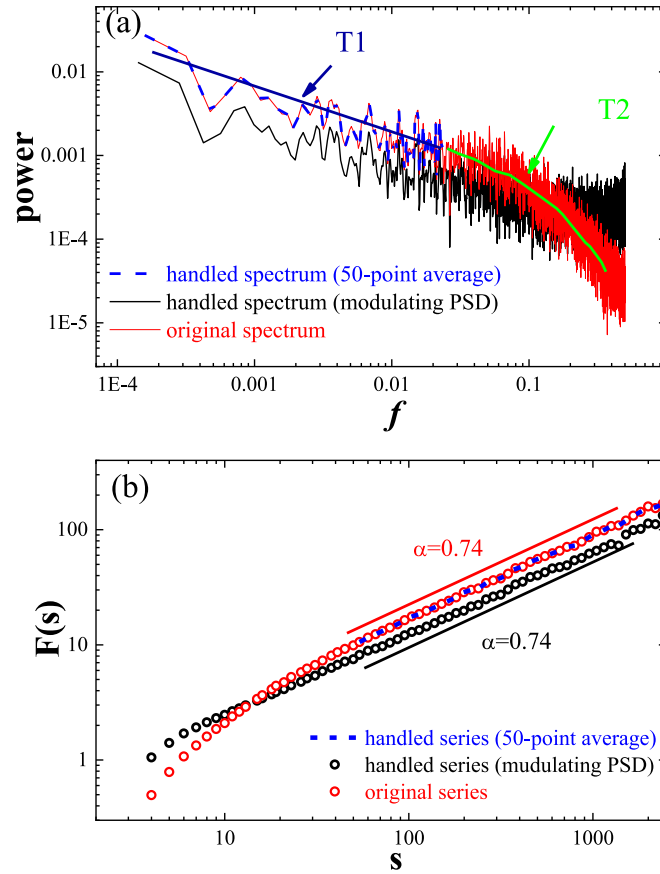


Fig. 2. Procedure to eliminate STC. (a) PSD of 50-point averaged series (blue dash line), modulated PSD (black) and PSD of raw series (red), (b) DFA for 50-point averaged series (blue dash line), modulated series (black) and raw series (red). (For interpretation of the references to color in this figure legend, the reader is referred to the web version of this article.)

Spearman correlation coefficient S [20] of series $\{x_t\}$ and $\{k_t\}$ (k_t is degree number of the node corresponding to x_t), which measures the strength between the original series and its degree series.

These three TPs chosen here are due to their essential quantifying ability of the topological features [31] and their links with ordinal information hidden in the original series. According to Manshour's study [20], series with low DFA exponents, and their HVGs are highly assortative [6]. As for e_{max} and S , they can quantify the variation of nodes' degree in more details than degree distribution, such as ordinal information in degree series [20]. When the analyzed time series is white noise, r , e_{max} and S reach their maximum values in our research (0.83, 8.7 and 0.23, respectively). For better comparison among these parameters, all values of TPs are normalized to the range [0, 1] by dividing their maximum values (0.83, 8.7 and 0.23).

2.2.2. Modeling and detection for idealized LTM

After calculating the above three TPs, we employ detrended fluctuation analysis (DFA) [11] to estimate LTM of a given time series $\{x_t\}$, and then use scatterplots to demonstrate the relation between LTM and TPs. Steps of DFA algorithm can be outlined as follows: (1) calculate the profile: $y_t = \sum_{k=1}^t (x_k - \bar{x})$, and $\bar{x} = \frac{1}{N} \sum_{k=1}^N x_k$; (2) for selected time scale S , divide $\{y_t\}$ into K intervals ($K = \lfloor N/S \rfloor$, " $\lfloor \cdot \rfloor$ " represents rounding down) and fit the quadratic or higher trend p_t in every intervals, then calculate the detrended profile: $z_t = y_t - p_t$; (3) calculate fluctuation function: $F^2(S) = \frac{1}{K} \sum_{v=1}^K (1/S \sum_{t=(v-1)S}^{vS} z_t^2)$; (4) fit DFA curve to derive the DFA exponent α according to the scaling law: $F(S) \propto S^\alpha$ [9].

For idealized reference, autoregressive fractionally integrated moving average, a widely used stochastic model is employed here [32,33]. The acronym "FARIMA" is often used, although it is also conventional to simplify the "FARIMA(p, d, q)" notation for models with p the order of the autoregressive model, d the degree of differencing (it can take the fractional values), and q the order of the moving-average model. We can generate time series with pure LTM by FARIMA (0, d , 0), in which $d = \alpha - 0.5$. And we can also control the STC and LTM of an idealized time series by FARIMA (1, d , 0).

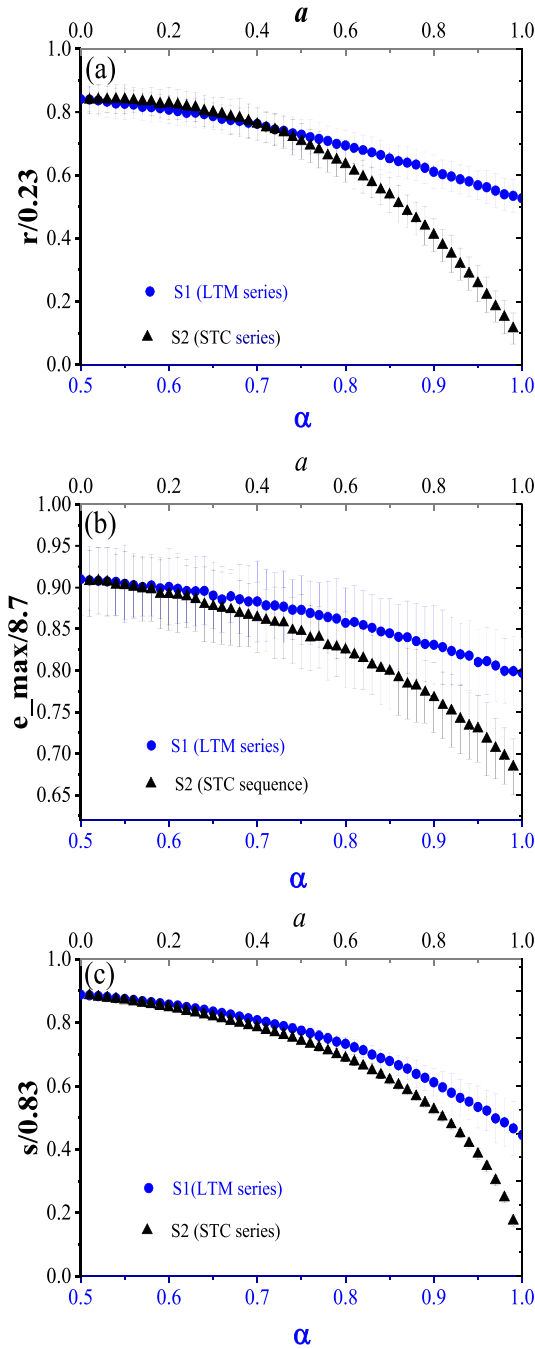


Fig. 3. Variations of normalized TPs with LTM strength α and STC strength a for S1 (idealized LTC processes) and S2 (pure short-term correlated time series). (a) r , (b) e_{max} , (c) S (The error bars around the dots are 99% confidence intervals, calculated from 100 samples). (For interpretation of the references to color in the text, the reader is referred to the web version of this article.)

2.2.3. Nonlinear correlation analysis

To quantify the nonlinear correlation in a time series $\{x_t\}$, the increment series method [22,34] can be adopted to calculate the correlation exponent α_m in the magnitude series $\{|x_{t+1} - x_t|\}$ by DFA, and if $0.5 < \alpha_m < 1$, it can be sure that $\{x_t\}$ has nonlinear correlation structures. And phase randomized surrogate (PRS) procedure [35,36] can be used to test and eliminate the effect of this nonlinear correlation. PRS procedure is outlined as follows: (1) preserve the Fourier amplitude of original time series $\{x_t\}$, but replace its Fourier phase by Fourier phase of white noise; (2) after replacing the Fourier phase, use

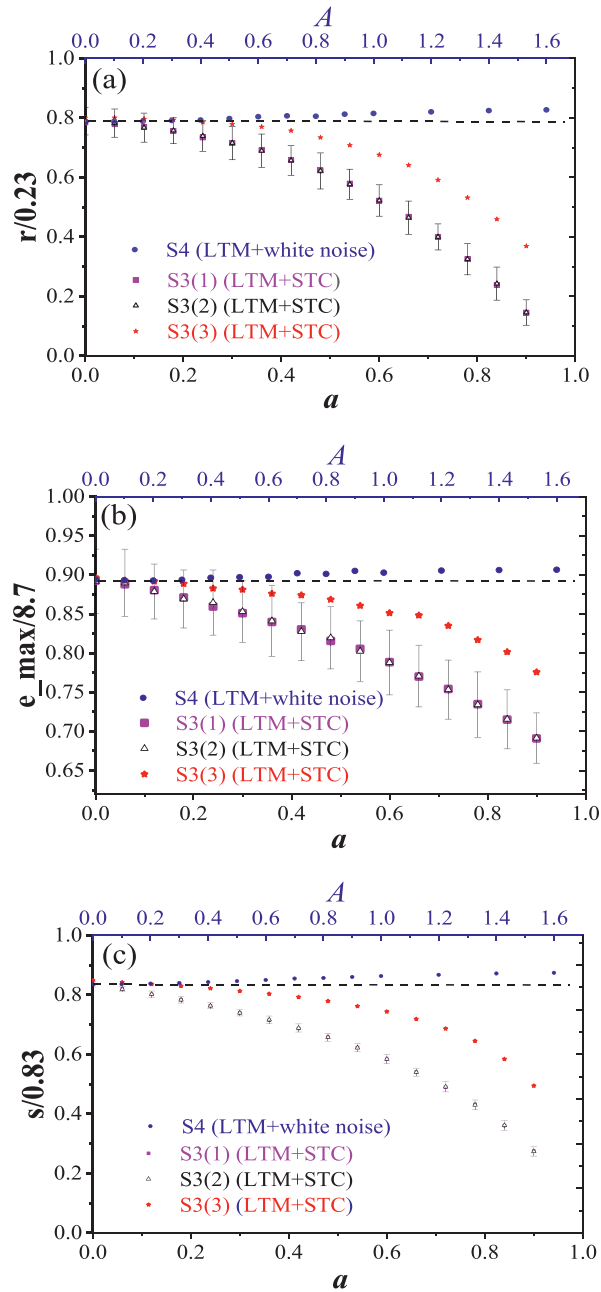


Fig. 4. Variations of normalized TPs of S3 (LTM processes with mixed STC) and S4 (LTM processes with mixed white noise) with STC strength a and noise strength A . Increasing a leads TPs decreasing, whereas increasing for increasing A . (a) r , (b) e_{max} , (c) S (The error bars around the dots are 99% confidence intervals, calculated from 100 samples, with black dash horizontal line as reference to show the variations of TPs clearly).

inverse Fourier transformation to reach a new sequence $\{x'_t\}$, in which the nonlinear correlation in the original time series $\{x_t\}$ will be eliminated in this procedure.

2.2.4. Eliminating influence of STC

As for STC of $\{x_t\}$, it can be taken as an autoregressive process of the first order (AR(1) process), and the interfering parameter can be calculated as the following [36]:

$$a = \frac{\langle x_{t-1}x_t \rangle}{\langle x_t x_t \rangle}, \quad (3)$$

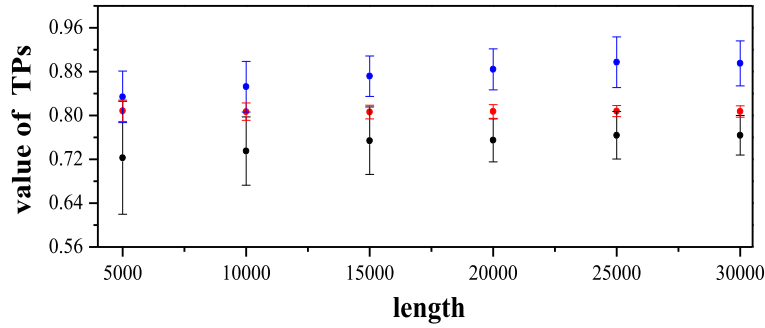


Fig. 5. Length effect on TPs calculation, r (blue), e_{max} (black) and S (red) (The error bars around the dots are 99% confidence intervals, calculated from 100 samples). All the time series are generated by FARIMA (0, 0.2, 0). (For interpretation of the references to color in this figure legend, the reader is referred to the web version of this article.)

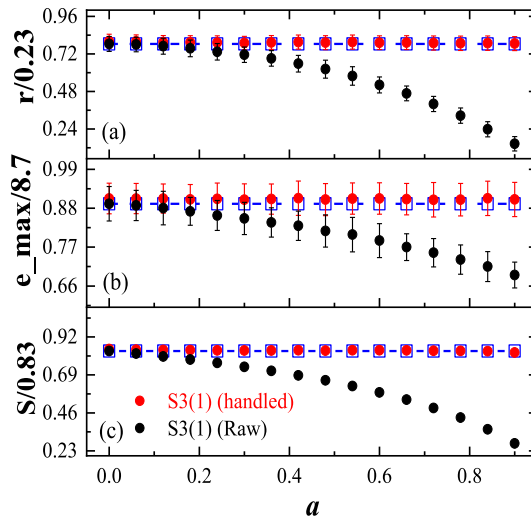


Fig. 6. Variations of normalized TPs for raw S3(1) (LTM processes $\alpha = 0.7$ with mixed STC) and handled S3(1) with different STC strengths. (a) r , (b) e_{max} , (c) S (The error bars around the dots are 99% confidence intervals, calculated from 100 samples, open blue boxes and blue dash lines are theoretical TPs results for pure LTM processes with $\alpha = 0.7$).

in which the value of a represents the strength of STC. For these temperature series, we eliminate STC by employing power spectrum density (PSD). To calculate the PSD of a given time series, one needs to calculate its Fourier spectrum and to do some de-noising procedures [10,36], then to get the power E at each frequency f , which follows $E(f) \propto f^\beta$ ($\beta = 2\alpha - 1$, β is PSD exponent and α is DFA exponent). Similar to result from DFA (see Fig. 2b), there is a crossover when STC exists (see the red curve in Fig. 2a). See Fig. 2a, in the PSD curve we first fit the trend (T1) over low frequency band and the trend (T2) over high frequency band respectively, they are different regimes. We have two choices to handle T2: (1) replacing T2 by T1 in high frequency band to modulate the PSD (see the black curve in Fig. 2a); (2) employing the multipoint average for the original series, to remove the frequency band corresponding to T2 [37] (see the blue dash line in Fig. 2a), but this method requests to reduce data length of the series largely. Then the modulated PSD is transformed back to time domain by inversed Fourier transformation without STC (see the black curve in Fig. 2b). It should be noted, modulating the PSD is only for testing if we could obtain a reliable/unaffected relation between TPs and LTM when STC and LTM coexist, and this does not mean that we aim to make the DFA scaling range wider. The above two choices could both help with our test, but in order to keep data length the same, we tend to select the first choice.

3. Results

3.1. Experiments on synthetic time series

3.1.1. Ability of complex network to infer LTM

To estimate LTM of a time series by means of complex network approach, time series should be mapped onto a network by HVG algorithm [28]. From this constructed network, three topological parameters (TPs) such as assortativity coefficient (r) [29], maximum Eigenvalue of adjacent matrix (e_{max}) [30], Spearman coefficient (S) [20] between time series and their

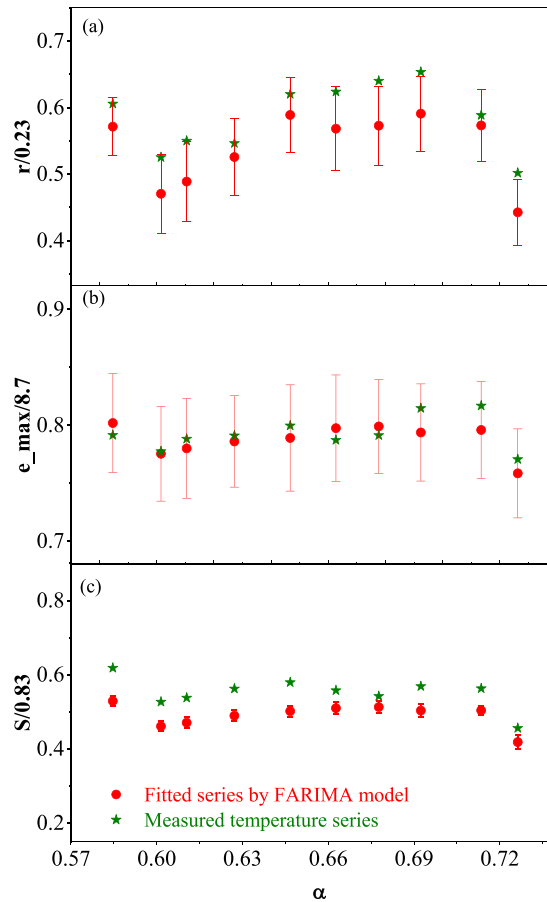


Fig. 7. Comparison of variations of normalized TPs with LTM strength α between temperature series (stars) and their corresponding outputs (dots) from FARIMA (1, d, 0). (a) r , (b) e_{max} , (c) S (The error bars around the dots are 99% confidence intervals, calculated from 100 samples).

degree sequences, will be calculated. For each kind of TPs, different values can quantitatively depict different network states [31], which are considered to represent the topological characteristics of network [20]. Manshour [20] found these three TPs can infer LTM information of fractional time series. However, STC and LTM often coexist in the real-world time series. We guess that both the two kinds of correlations can change TPs of HVG, but this has not been showed in the past studies. Firstly, two kinds of sequences is generated as fellows, and their three TPs are also calculated:

- S1: LTM series: generated by the model FARIMA (0, d, 0) [32] ($\alpha = 0.5 + d$, α is the DFA exponent and represents the strength of LTM);
- S2: STC sequence: generated by the model AR(1) process ($x_i = ax_{i-1} + \varepsilon_i$, ε_i is white noise, a represents the strength of STC);

In Fig. 3, the blue dotted lines show that the three TPs all change with the strength of LTM. When α increases, the corresponding TPs all monotonously decrease. In that case, these one-to-one relations between LTM strength and TPs might be used to further estimate LTM of other time series. However, the black dotted lines in Fig. 3 show that strength of STC (a) can also alter the value of TPs. When a becomes stronger, the decreasing rates of all three TPs are even more dramatically than LTM. That is to say, it is possible for STC to influence the estimation of LTM. However, these are only concluded from simple conditions, and it is more important to know how STC affects the estimation of LTM when they are present in the times series at the same time.

3.1.2. Impact of STC on estimating LTM

In the real world time series, LTM and STC usually coexist, and they are not easy to be separated from each other. When LTM and STC coexist, the estimation of LTM often requires certain specific handling. Just like Fig. 1b, taking daily temperature series as an example, there exists a crossover around $s = 14$ in their DFA curves [11,12], which is taken to be induced by STC apart from LTM. In this case, the DFA exponent must be extracted in specific interval to avoid the crossover [12,13]. For temperature series, the LTM represents low-frequency climate variability [12], which is regarded as the intrinsic

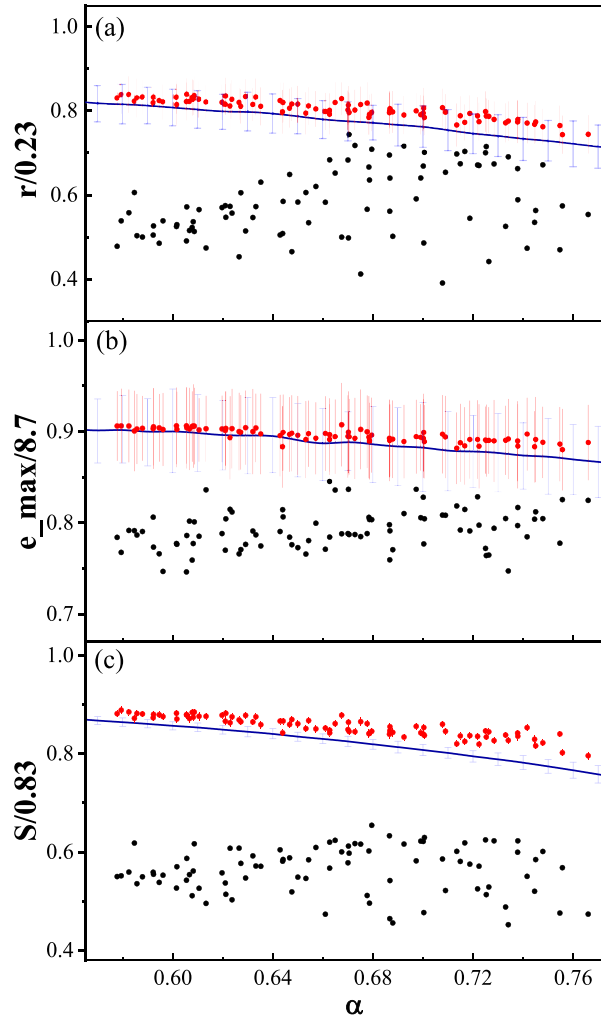


Fig. 8. Comparison of variations of normalized TPs with LTM strength α from idealized LTM processes (blue lines) with those from mean air temperature anomaly series (black dots) over China stations and the handled temperature series (red dots). (a) r , (b) e_{max} , (c) S (The error bars around the dots are 99% confidence intervals, calculated from 100 samples). (For interpretation of the references to color in this figure legend, the reader is referred to the web version of this article.)

feature of a climate system, but climate noises [6] (originated from some weather systems) can induce STC meanwhile. Such coexistence of LTM and STC is common for many other natural time series as well [3,4,31], so to quantify how STC affect the LTM estimation is necessary. Here we construct another three time sequences to model the temporal structures with LTM and STC:

- S3(1): Set the targeted sequence as $x_i = \alpha x_{i-1} + \xi_i$ [37], in which $\{\xi_i\}$ is the sequence of S1;
- S3(2): Use FARIMA (1, d , 0) to generate the targeted sequence directly;
- S3(3): Set the targeted sequence $x_i = y_i + \xi_i$, in which $\{y_i\}$ is the sequence of S2, and $\{\xi_i\}$ is the sequence of S1 (normalization was performed in advance);

For S3(1)–S3(3), we keep that LTM strengths of them are equal to a constant (e.g. $\alpha = 0.7$) but the STC strengths of them are variable, see Fig. 4. With the same LTM (the same value of α), TPs apparently decrease when STC (a) becomes stronger. It shows that existence of STC will make the values of TPs smaller, which will overestimate the strength of LTM by TPs of HVG. In addition, S3(1) and S3(2) nearly collapse with the similar uncertainties.

3.1.3. Impact of white noises on estimating LTM

From Fig. 4, it's sure that other inherited information can really influence the estimation of LTM by TPs of HVG. Since the measured noise is inevitable in the real world time series, it is necessary to check how superposition of white noise influences the TPs of HVG in a given time series with given LTM. We construct the sequences S4 to model this case:

S4: Let the targeted sequence $x_i = A\varepsilon_i + \xi_i$, in which $\{\varepsilon_i\}$ is white noise. $\{\xi_i\}$ is the sequence of S1, and the value of A represents how much white noise has been added (normalization was performed in advance).

Then the three TPs of S4 are calculated and displayed in Fig. 4, in which $A = 0$ represents the estimated LTM is free from white noise, but $A > 0$ represents different magnitudes of added white noise. It is obvious that when more and more white noise is added (A becomes larger), there exists a little bit increasing trend in the variation of each TP. Also, the confidence intervals should be noted in Fig. 4a and b, where white noise will increase the uncertainties of the calculation for both r and e_{max} .

In addition, the effect from data length is minor on the estimations of the three TPs (Fig. 5). When the series length is larger than 15,000, mean values and confident intervals of the three TPs all reach their saturated levels (each series analyzed in this article has nearly 20,000 data points).

3.2. Could we obtain the unaffected relation between TPs and LTM?

In the above it's demonstrated that STC is the main factor to influence LTM estimation by HVG, meanwhile TPs of HVG are robust to white noise and data length. So could we using a reasonable processing to eliminate the influence of STC? We carried out the processing mentioned in Section 2.2.4 (modulating the PSD) to the synthetic time series with known mixed correlations, see S3(1), if this handling works, we will recover the inherent associations between LTM of pure long-range correlated time series and TPs of their HVG networks from idealized stochastic time series. Both results for r and S are totally in excellent agreement with the expected ones (see Fig. 6a and c), only results for e_{max} are a little bit departure from the mean values as expected, but still in the confidence intervals (see Fig. 6b). That is to say, after appropriate handling, LTM of synthetic time series with mixed correlation can really be extracted by TPs of HVG.

We also tested if multipoint average is helpful to acquire the better relation between LTM and TPs, and the same results as Fig. 6 could be observed. But multipoint average proceeding requested much longer data length for the original series. Compared with modulating the PSD, multipoint average proceeding makes the PSD or DFA curve even shorter as Fig. 2 shows. That's to say, the width of scaling range doesn't influence the relation between LTM and TPs, but the regime of STC does and should be eliminated.

3.3. Application in real-world complex time series

3.3.1. What properties of temperature series dominate the values of TPs?

The above results indicate that the variations of TPs can be mostly explained by the changing strength of both LTM and STC. Will this case also happen for the temperature anomaly series from the real world?

We randomly choose 10 temperature series from the raw anomaly data referred in Fig. 1a, and then fit each one of them with FARIMA (1, d, 0) process (both of LTM and STC can be included in this model). For each temperature series, both DFA exponent α and STC strength a are calculated. At the same time, in FARIMA (1, d, 0), the corresponding model parameters are determined by these calculated α and a . Fig. 7 shows TPs' variations with α for these raw time series and corresponding fitted ones from FARIMA (1, d, 0) model. For e_{max} , the results of raw temperature series all locate in the confidence intervals of fitted model series, and their mean values have similar decreasing trends. For r , there are similar results as e_{max} , apart from 4 closed to their upper limited values. But it is a little different for S , the values of S from raw temperature series are all larger than those from fitted model, which may be caused by the nonlinear correlations in the raw temperature series (see Fig. 1(c), $\alpha_m > 0.5$ represents marked nonlinearity, see Methods) or other nonlinear temporal structures in temperature series, such as irreversibility [38], multifractality [39] and asymmetry [40], but they are not explained in the fitted FARIMA model.

3.3.2. Inferring LTM of daily air temperature series from TPs of their HVG

Daily anomaly air temperature series are from climate systems with different dynamics over different scales, besides LTM, there are still different dynamic components including white noise, STC and nonlinear dynamics. In order to infer LTM of daily air temperature series from TPs of their HVG, some preprocessing treatments must be carried out. Since the variations of TPs can be mostly explained by the changing strength of both LTM and STC, and we first eliminate the effect of STC, which can be done by the modulated PSD (as Section 2.2.4 shows). At the same time, nonlinear feature such as nonlinear correlations should be also removed from the raw series, which can be carried out by phase randomized surrogate (PRS) procedure. After modulated PSD and PRS manipulating, the generated daily anomaly air temperature series are called handled series, in which both STC and nonlinear correlation have been removed.

There are nearly the same variations of e_{max} for handled series and fitted series from FARIMA (0, d, 0) (see Fig. 8b), which are all markedly different from those for raw series. The agreement of handled series and fitted series from FARIMA (0, d, 0) with LTM only for r is also acceptable in the confidence intervals (see Fig. 8c), apart from a little bit overestimation for stronger LTM due to measured noise (see Fig. 4a). Only the results of handled series for S are still a little higher than those of fitted series from FARIMA (0, d, 0) with LTM only (see Fig. 8c), which is due to much higher sensitive to noise (see Fig. 4c).

4. Conclusions and discussions

From the artificially generated stochastic series with known LTM, STC and/or Mixed LTM and STC, it is found that both LTM and STC can change values of TPs from HVG of time series. However, these inherent associations between LTM of time series and TPs of their HVG can be indeed recovered after suitable preprocessing procedures (see Figs. 2 and 6), and these one to one monotonic relations can be taken to infer the LTM from the corresponding estimated values of TPs. Our results also indicate that LTM in time series can be inferred by means of the inherent associations between LTM of pure long-range correlated time series and TPs of their HVG.

There are different dynamics ranging from white noise, STC to some period or chaotic dynamics [24] in the real world time series, so the inherent associations between LTM of pure long-range correlated time series and TPs of their HVG can't be directly employed to infer the LTM in the real world time series, suitable preprocessing procedures must be carried out to eliminate these mixed components. Preprocessing procedures include modulated PSD that can be applied to eliminate the influence from STC, and PRS that works well in removing the nonlinear correlations in the time series. Some other filtering procedures maybe also work well in eliminating influence of STC, for example multipoint (biweekly) average could be considered [37] when data length of the original series is long enough.

For a given time series from the real world, the following steps are recommended to accurately infer LTM by means of the inherent associations between LTM and TPs of its HVG:

- 1) Making Fourier transformation to this given time series to get the Fourier spectrum and phase;
- 2) Checking if there is different trends or regimes in a log-log coordinate of the Fourier spectrum, then making Fourier spectrum's high frequencies band having the same trend as low frequencies (or using multipoint average to remove the different regime in high frequencies band). In this step, the influence of STC on TPs' relations will be removed;
- 3) Replacing the Fourier phase in modulated Fourier spectrum with Fourier phase of white noise, in this step, nonlinear correlation in the original series will be removed through PRS operations;
- 4) For the new Fourier spectrum and phase, using inverse Fourier transformation to get a new time series and calculating its corresponding TPs;
- 5) Repeating the steps 3–4 for given times, such as 100 times or 1000 times (in order to determine each TP precisely, TP value beyond certain threshold, such as two standard deviation of each TP, should be discarded) and calculating the mean value of TPs;
- 6) Fitting the one-to-one relation between TPs and LTM from the pure long-range correlated time series;
- 7) Employing the mean value of TPs and the fitted function relation to infer the LTM of time series.

We want to point out that the sensitivity of different TPs is different for effect of dynamics such as white noise, STC and some period or chaotic dynamics. Optimized TP can be chosen to infer LTM in the real world time series by means of the inherent associations between LTM of pure long-range correlated time series and TPs of their HVG, and this deserves further studies, which might be since of: (1) in the calculation of TPs, it's not required to determine scaling range as DFA method, larger uncertainties in deriving the LTM exponent by DFA might be weakened. (2) The real-world time series might be mixed with some unperceived regimes such as STC [12], large-scale or small-scale nonlinear structures [13,34] and residual period signal [15]. These will induce the tiny distortion for the DFA curves. The DFA curves might be not noticed to be distorted without detailed checking, at that time the slope or DFA index might be inaccurate. But for TPs, as the blue curves showed in Fig. 8, widths of their variations with LTM are respectively determined and narrow. If the above unperceived regimes exist in time series, values of TPs will deviate from this interval and be noticed in time, as the black dots in Fig. 8. So that the influence of some mixed regimes might be better noticed and even avoided by employing TPs. (3) Complex network approaches to time series attract much attention [16–18] since of its powerful detection for system features, good robustness to white noise, and limited data length that is also demonstrated in Section 3.1.3 of this paper.

Acknowledgments

We thank the anonymous reviewers for their important suggestions to improve this article. We also thank Dr. Lichao Yang for her detailed corrections and helpful suggestions to improve this paper's organization and expression. We acknowledge the supports from National Natural Science Foundation of China (Nos. 41175141, 41475048).

References

- [1] Mandelbrot BB, Wallis JR. Some long-run properties of geophysical records. *Water Resour* 1969;5:321–40.
- [2] Kim HF, Ghazizadeh A, Hikosaka O. Dopamine neurons encoding long-term memory of object value for habitual behavior. *Cell* 2015;163(5):1165.
- [3] Bursa N, Tatlıdil H. Investigation of credit default swaps using detrended fluctuation analysis which is an Econophysical technique. *Eurasian Econom Stat Empr Econ J* 2015;2:25–33.
- [4] O'Connell PE, Koutsoyiannis D, Lins HF, et al. The scientific legacy of Harold Edwin Hurst (1880–1978). *Hydrol Sci J* 2016;61(9):1571–90.
- [5] Franzke C, Yuan N. Why is scaling important? *Centenn Millenn Clim Var* 2017;25(3):134–5.
- [6] Franzke CL, Osprey SM, Davini P, Watkins NW. A dynamical systems explanation of the Hurst effect and atmospheric low-frequency variability. *Sci Rep* 2015;5:9068.
- [7] Lennartz S. Long-term memory in climate records and the detection problem. *Nature* 2010;5471:166.
- [8] Ray R, Khondekar MH, Ghosh K, Bhattacharjee AK. Memory persistency and nonlinearity in daily mean dew point across India. *Theor Appl Climatol* 2016;124(1–2):119–28.

- [9] Kantelhardt JW, Koscielny-Bunde E, Rego HHA, et al. Detecting long-range correlations with detrended fluctuation analysis. *Phys A* 2001;295(3):441–54.
- [10] Talkner P, Weber RO. Power spectrum and detrended fluctuation analysis: application to daily temperatures. *Phys Rev E* 2000;62(1):150–60.
- [11] Kiraly A, Janosi IM. Stochastic modeling of daily temperature fluctuations. *Phys Rev E* 2002;65:051102.
- [12] Höll M, Kantz H. The fluctuation function of the detrended fluctuation analysis: investigation on the AR(1) process. *Eur Phys J B* 2015;88(5):1–9.
- [13] Höll M, Kantz H. The relationship between the detrended fluctuation analysis and the autocorrelation function of a signal. *Eur Phys J B* 2015;88:327.
- [14] Lennartz S, Bunde A. Eliminating finite-size effects and detecting the amount of white noise in short records with long-term memory. *Phys Rev E* 2009;79:066101.
- [15] Deng Q, Nian D, Fu Z. The impact of inter-annual variability of annual cycle on long-term persistence of surface air temperature in long historical records. *Clima Dyn* 2018;50:1091–100.
- [16] Lacasa L, Luque B, Ballesteros F, et al. From time series to complex networks: the visibility graph. *PNAS* 2008;105(13):4972–5.
- [17] Donner RV, Donges JF. Visibility graph analysis of geophysical time series: potentials and possible pitfalls. *Acta Geophys* 2012;60(3):589–623.
- [18] Zou Y, Donner RV, Marwan N, Donges JF, Kurths J. Complex network approaches to nonlinear time series analysis. *Phys Rep* 2018.
- [19] Weng T, Zhao Y, Small M, et al. Time-series analysis of networks: exploring the structure with random walks. *Phys Rev E* 2014;90(2):022804.
- [20] Manshour P. Complex network approach to the fractional time series. *Chaos* 2015;25(10):103105.
- [21] Rodríguez MA. Relating the large-scale structure of time series and visibility networks. *Phys Rev E* 2017;95(6–1):062309.
- [22] Kalisky T, Ashkenazy Y, Havlin S. Volatility of linear and nonlinear time series. *Phys Rev E* 2005;72(1):011913.
- [23] Franzke CL. Nonlinear Trends, Long-range dependence, and climate noise properties of surface temperature. *J Climate* 2011;25(12):1487.
- [24] Weng T, Zhang J, Small M, et al. Memory and betweenness preference in HVGs induced from time series. *Sci Rep* 2017;7:41951.
- [25] Zhang R, Zou Y, Zhou J, et al. Visibility graph analysis for re-sampled time series from auto-regressive stochastic processes. *CNSNS* 2017;42:396–403.
- [26] Donges JF, Donner RV, Kurths J. Testing time series irreversibility using complex network methods. *Euro Phys Lett* 2012;102(1):381–92.
- [27] Xie F, Fu Z, Piao L, Mao J. Time irreversibility of mean temperature anomaly variations over China. *Theor Appl Clima* 2016;123:161–70.
- [28] Luque B, Lacasa L, Ballesteros F, et al. Horizontal visibility graphs: exact results for random time series. *Phys Rev E* 2009;80:046103.
- [29] Newman ME. Assortative mixing in networks. *Phys Rev Lett* 2002;89(20):208701.
- [30] Rowlinson P. The largest eigenvalue of a graph: a survey. *Linear Multilinear Algebra* 1990;28(1–2):3–33.
- [31] Newman M. *Networks: an introduction*. Oxford University Press; 2010.
- [32] Granger CW, Joyeux R. An introduction to long-memory time series models and fractional differencing. *J Time Ser Anal* 1980;1(1):15–29.
- [33] Massah M, Kantz H. Confidence intervals for time averages in the presence of long-range correlations: a case study on earth surface temperature anomalies. *Geophys Res Lett* 2016;43(17):9243–9.
- [34] Fu Z, Shi L, Xie F, et al. Nonlinear features of Northern Annular Mode variability. *Phys A* 2016;449:390–4.
- [35] Theiler J, Eubank S, Longtin A, et al. Testing for nonlinearity in time series: the method of surrogate data. *Phys D* 1992;58(92):77–94.
- [36] Duchon C, Hale R. *Time series analysis in meteorology and climatology*. West Sussex: John Wiley & Sons, Ltd; 2012.
- [37] Fu Z, Xie F, Yuan N, et al. Impact of previous one-step variation in positively long-range correlated processes. *Theor Appl Climatol* 2016;124(1–2):339–47.
- [38] Stone L, Landan G, May RM. Detecting time's arrow: a method for identifying nonlinearity and deterministic chaos in time-series data. *Proc R Soc B* 1996;263(1376):1509–13.
- [39] Ashkenazy Y, Baker DR, Gildor H, et al. Nonlinearity and multifractality of climate change in the past 420,000 years. *Geophys Res Lett* 2003;30(22):2146.
- [40] Bartos I, János IM. Atmospheric response function over land: strong asymmetries in daily temperature fluctuations. *Geophys Res Lett* 2005;32(23):113–33.